

# THE SENSITIVITY OF MULTI-FREQUENCY (X, C AND L-BAND) RADAR BACKSCATTER SIGNATURES TO BIO-PHYSICAL VARIABLES (LAI) OVER CORN AND SOYBEAN FIELDS

Xianfeng Jiao, Heather McNairn, Jiali Shang and Jianguo Liu  
Agriculture and Agri-Food Canada, 960 Carling Ave., Ottawa, Ontario K1A 0C6

**Key words:** Agriculture, Crop, Analysis, SAR, Multifrequency

## ABSTRACT:

The objective of this study is to investigate the sensitivity of synthetic aperture radar (SAR) backscatter signatures to crop bio-physical variables. The experimental data were collected over corn and soybean fields in eastern Ontario (Canada) during the 2008 growing season. Remote sensing acquisitions consisted of TerraSAR-X dual-polarized stripmap data (X-band), RADARSAT-2 Fine beam quad-polarized data (C-band) and ALOS PALSAR dual-pol data (L-band), as well as the Compact Airborne Spectrographic Imager (CASI) and SPOT-4 multi-spectral data. Plant variables, such as leaf area index (LAI) and surface volumetric soil moisture were measured to coincide with these acquisitions and key phenological growth stages. Analyses were conducted based on statistical correlation and a simple backscatter process model (the water cloud model). The results of this study show that the lower frequency bands, such as L and C, were closely related with LAI. For both corn and soybean crops, most C-band linear (HH, VV, HV) backscatter coefficients were correlated with LAI; backscatter increased with increasing LAI. L-band backscatter at HH and HV polarizations produced the highest correlations with corn LAI ( $r=0.90-0.96$ ). Conversely, these L-band polarizations were only weakly correlated with soybean LAI. The higher frequency X-band was poorly correlated with both corn and soybean LAI. Based on these findings, the water cloud model was used to express C-band and L-band backscatter for the whole canopy as a function of LAI and surface soil moisture.

## 1. INTRODUCTION

The monitoring of crop bio-physical variables is a very important task in agricultural management and in yield forecasting. Information from satellites can be exploited to assist in estimating key crop growth indicators including Leaf Area Index (LAI), biomass and crop height. LAI is an important indicator of agricultural productivity and a critical variable in crop growth models. Optical remote sensing data have been used to estimate LAI (Baret and Guyot, 1991; Brown et al., 2000; Chen and Cihlar, 1996). However, operational productivity and yield monitoring activities that rely solely on optical imagery are vulnerable to data gaps during critical crop growth stages as a result of unfavourable atmospheric conditions. Synthetic aperture radars (SARs) are unaffected by atmospheric haze and clouds. In addition to this oft-quoted advantage, SAR data also provide complementary and unique characterizations of vegetation when compared with the information provided by optical imagery.

SAR response is dependent upon the sensor configuration including incidence angle, frequency and polarization. Target characteristics, most notably the soil and crop dielectric and geometric properties, influence scattering behaviour and the magnitude of the radar backscatter. Shorter SAR wavelengths such as X-band (~3 cm) and C-band (~6 cm) interact mainly with the top part of the canopy layers while long wavelengths such as L-band (~20 cm) have a greater penetration depth, interacting with the entire crop canopy and resulting in greater scattering contributions from the soil (Ulaby et al., 1984). Penetration depth depends on whether the bio-physical parameters of the scatters within a vegetation layer (e.g., canopy water content, size and geometry of the canopy components) scatter or attenuate the incident microwaves. Inoue *et al.* (2002) compared backscatter responses from multi-frequency (Ka, Ku, X, C, and L) data in the context of several bio-physical variables of paddy rice. The results showed that

LAI was best correlated with HH- and cross-polarization backscatter at C-band, while fresh biomass was best correlated with HH- and cross-polarizations at L-band. Conversely, the higher frequency bands (Ka, Ku, and X) were poorly correlated with LAI and biomass.

Many experimental studies have linked the bio- and geo-physical characteristics of crops with backscatter recorded by SAR sensors. (Clevers and van Leeuwen, 1996; Ferrazzoli et al., 1999; McNairn, 2002; Taconet et al., 1996). Most of these studies were carried out using C-band SAR due to the availability of this radar frequency on the first generation of satellite SAR sensors (ERS-1/2, RADARSAT-1). The SAR sensors currently operational include TerraSAR-X (X-band), COSMO-SkyMed (X-band), PALSAR/ALOS (L-band), ASAR/ENVISAT (C-band), RADARSAT-1/2 (C-band), and ERS-2 (C-band). With access to such a wealth of SAR satellites, it is now possible to study the sensitivity of multi-frequency and multi-polarization data to LAI through the entire crop growth cycle. Detailed understanding of radar response to crops characteristics as a function of SAR parameters (wavelength, incidence, and polarization) is the first essential step in developing robust methods to retrieve crop bio-physical variables such as LAI.

This study investigates the sensitivity of TerraSAR-X, PALSAR/ALOS, and RADARSAT-2 to crop bio-physical variables. The objective is to assess the radar response of corn and soybean crops with respect to radar wavelength (X, C, and L-bands) and polarization. Leaf area index (LAI) and surface volumetric soil moisture were measured to coincide with remote sensing acquisitions. In this paper, correlation analyses were conducted between radar backscatter and LAI. In addition, a semi-empirical backscatter process model (the water cloud model) was used to develop the relationship between SAR backscatter and target conditions, including LAI and soil moisture.

## 2. STUDY SITE AND DATA COLLECTION

Two sites were selected near Ottawa, Ontario, Canada for field and satellite data collection, the Canadian Food Inspection Agency (CFIA) research farm and a region of private producers east of Casselman, Ontario. The terrain across these two study sites can be considered level to very gently sloping (<2%) with an average field size of 23 hectares. This region of eastern Canada consists largely of corn and soybean annual crop production.

Ground truth measurements were performed on several selected sites. Within the CFIA site, 13 fields including 16 corn and 21 soybean sample sites were selected. At the Casselman site, 20 fields including 10 corn and 10 soybean sample sites were visited. Total LAI was measured at each sample site using an LAI-2000 (Li-Cor, Inc., Lincoln, NE) plant canopy analyser throughout the growing season. Volumetric surface soil moisture was measured coincident with each SAR acquisition, using Delta-T Theta probes with 6-cm waveguides. At each site, mean soil moisture was calculated from ten replicate moisture measurements.

SAR images were acquired by TerraSAR-X, PALSAR/ALOS, and RADARSAT-2 satellites. During the 2008 growing season, two RADARSAT-2 Fine beam mode quad-pol images (July 6 and 9) and one PALSAR/ALOS (July 2) were acquired over the CFIA site; two RADARSAT-2 Fine beam mode quad-pol images (August 23 and August 26) and one TerraSAR-X stripmap image (August 21) were acquired over the Casselman site. The pixel spacing of TerraSAR-X, PALSAR/ALOS, and RADARSAT-2 is 3 m, 12.5 m and 8 m, respectively. Characteristics of the SAR images used in this study are summarized in table 1.

Date	SAR sensor	mode	pol.	incident angle
07-02-2008	PALSAR	L1.5	HH,HV	34°
05-23-2007	PALSAR	L1.5	HH,HV	21°
07-09-2008	Radarsat-2	FQ20	Quad-pol	40°
07-06-2008	Radarsat-2	FQ6	Quad-pol	26°
08-21-2008	TerraSAR-X	stripmap	HV/VV	44°

Table 1. Main characteristics of SAR images used in this study.

Optical images were acquired by the Compact Airborne Spectrographic Imager (CASI) and SPOT-4 multi-spectral satellite. CASI hyperspectral data were acquired on August 21, 2008 over the Casselman site. SPOT-4 multi-spectral data were acquired on July 6, 2008 over the CFIA site. From the CASI and SPOT-4 data, the Modified Triangular Vegetation Index (MTVI2) (Haboudane et al., 2004) was calculated. A non-linear curve fitting procedure was used to establish an empirical equation for LAI estimation from MTVI2 (Liu et al., 2009):

$$LAI = -6.247 \times \ln(0.946 - 0.643 \times MTVI2)$$

Using this formula, LAI maps for the entire study site were generated from the optical data, with an RMSE of 0.76 and an  $R^2$  of 0.85.

## 3. METHODOLOGY

### 3.1 Image processing

Radiometric calibration of TerraSAR-X and PALSAR/ALOS images was carried out using the follow equations. These equations were used to convert the digital number of each pixel  $DN_i$  into a backscatter coefficient ( $\sigma^0$ ).

For TerraSAR-X,

$$\sigma_i^0 (dB) = 20 \log_{10} DN_i + 10 \log_{10} (CalFact) + 10 \log_{10} (\sin(\theta_i))$$

CalFactor is given in the TerraSAR-X data delivery package annotation file. It is processor and product type dependent.

For PALSAR/ALOS,

$$\sigma_i^0 (dB) = 10 \log_{10} (DN_i^2) + CF$$

The calibration factor (CF) for PALSAR L1.5 products is -83 dB. The ALOS and TerraSAR data products were delivered in ground range. A 3 X 3 Enhance Lee filter was applied to both the ALOS and TerraSAR data to reduce speckle noise. RADARSAT-2 fine quad-pol SLC data were provided as compressed stokes matrix values for each slant range pixel. Prior to extracting the backscatter information, a boxcar filter with a 5 by 5 kernel size was applied to the polarimetric SAR scattering matrix data to suppress SAR speckle. After filtering the covariance matrix was converted to a symmetrized covariance matrix. From the symmetrized 3 by 3 covariance matrix, intensity backscatter (HH/HV/VV) was extracted. All the data were then geometrically corrected and geo-referenced using national road network vector data.

### 3.2 Water cloud model

The water cloud model was introduced first by Attema and Ulaby (1978). In the general version of the water cloud model, the power backscattered by the whole canopy ( $\sigma^0$ ) can be represented as the incoherent sum of contributions of the vegetation, ( $\sigma_{veg}^0$ ), and the underlying soil, ( $\sigma_{soil}^0$ ). This study selected the model modified by (Prévoit et al., 1993) as it incorporates LAI as a descriptor of vegetation development. In this model, SAR backscatter from a canopy at a given incidence angle can be written as:

$$\sigma^0 = AL^E \cos(\theta) (1 - \exp(-2BL / \cos(\theta))) + \sigma_{soil}^0 \exp(-2BL / \cos(\theta))$$

where  $\tau$  is the two-way attenuation through the canopy layer,  $L$  is the LAI, expressed in ( $m^2 m^{-2}$ ), the backscatter coefficients  $\sigma^0$ ,  $\sigma_{soil}^0$  and  $\sigma_{veg}^0$  are expressed in power units.  $A, B, C, D$  and  $E$  are model coefficients to be defined by experimental data.  $A, B$  and

E are parameters which depend on canopy type. E is a positive value. Parameters C and D are dependent on soil moisture.

#### 4. RESULTS AND DISCUSSION

Two dates of LAI maps (July 6 and August 21) were near-coincident with SAR acquisitions on July 2 (ALOS), July 6 (RADARSAT-2), July 9 (RADARSAT-2) and August 21 (TerraSAR). With LAI maps derived from optical data, LAI was estimated on a detailed pixel by pixel basis. Definiens software was then used to segment these maps into zones of homogeneous LAI for each corn and soybean field. These homogeneous zones were used as the primary sampling units. The average SAR backscatter and the mean LAI for each sampling unit were extracted for both corn and soybean crops.

##### 4.1 Correlation analysis between SAR data and LAI

To quantify the relationship between SAR backscatter and LAI, and to assess the sensitivity of SAR frequency and polarization to this crop growth parameter, correlation analyses were conducted. Scattering from within the crop canopy and the subsequent scattering back to the radar sensor is related to the physical structure of the scattering elements of the canopy, as well as their dielectric properties. Consequently a strong correlation between plant variables such as LAI and radar return has physical meaning. Table 2 provides the simple correlation analysis results for each SAR data set.

	Corn	Soybean
<b>PALSAR/ALOS</b>		
HH	0.92	0.28
HV	0.96	0.26
<b>RADARSAT-2 FQ20</b>		
HH	0.72	0.60
VV	0.79	0.73
HV	0.79	0.47
<b>RADARSAT-2 FQ6</b>		
HH	0.68	0.80
VV	0.72	0.62
HV	0.90	0.58
<b>TerraSAR-X</b>		
VV	-0.11	-0.20
HV	0.03	-0.65

Table 2. Simple correlation coefficients (r) between SAR data and LAI.

##### 4.1.1 SAR backscatter from corn crops

For corn, a strong correlation was found for both L-band and C-bands. The highest correlation coefficients ( $r=0.90-0.96$ ) were reported for L-HH and L-HV backscatter and for C-HV backscatter from the RADARSAT-2 FQ6 mode. Figure 1 plots L-HH, L-HV and C-HV (FQ6 mode) backscatter against corn LAI. Backscatter at these frequencies and polarizations were strongly linearly correlated with LAI. The coefficients of determination ( $R^2$ ) were 0.92, 0.85 and 0.80 for HV and HH at L-band and HV at C-band, respectively.

Slightly lower correlations ( $r=0.68-0.79$ ) were reported for corn for all C-band linear polarizations at the shallower RADARSAT-2 FQ20 mode, as well as for the linear like-polarizations (HH,VV) at the steeper RADARSAT-2 FQ6 mode. Backscatter at X-band was poorly correlated with corn LAI ( $r < 0.03$ ) regardless of polarization.

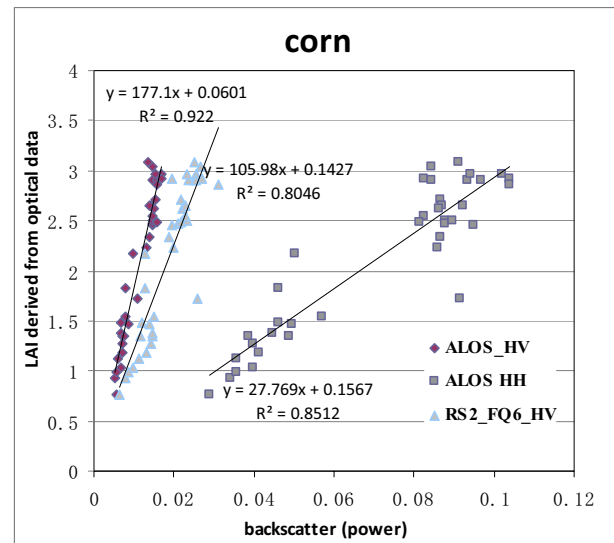


Figure 1 Correlation between L-HH, L-HV and C-HV (FQ6 mode) backscatter and corn LAI.

##### 4.1.2 SAR backscatter from soybean crops

For soybeans, SAR backscatter was only weakly correlated with LAI. The highest correlations were reported for the C-band data ( $r=0.58-0.80$ ). Backscatter from L-band and X-band had no significant correlation with LAI. Figure 2 illustrates the linear relationship between HH, VV and HV backscatter at C-band (RADARSAT-2 FQ6 mode) and LAI. The best correlations were observed for C-HH backscatter ( $R^2=0.63$ ).

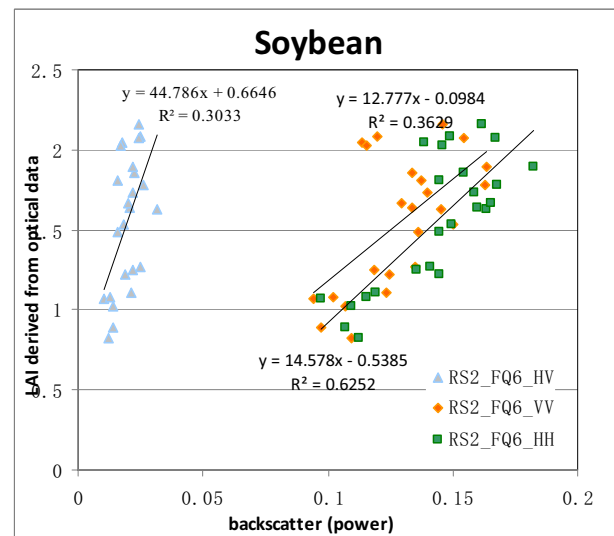


Figure 2 Correlation between C-band HH, VV and HV backscatter (RADARSAT-2 FQ6 mode) and LAI.

In summary, the lower frequencies such as L- and C-band were correlated with LAI, while the higher frequency X-band was poorly correlated. These results may be explained by the wavelength relative to the size of the crop scattering elements, but also by the difference in the canopy penetration. High frequency X-band provides little canopy penetration.

##### 4.2 Water cloud model

The backscatter signal from vegetated surfaces is affected by many factors, including the physical structure of the plants and the canopy (biomass, leaf size, stem density, LAI, etc.) as well as the surface volumetric moisture of the soil below the canopy.

Direct scattering from the canopy and the soil, as well as multiple interactions between the vegetation components and the soil, all contribute to the magnitude and scattering characteristics of the SAR response. Simple linear or non-linear expressions fail to adequately express the interaction of microwaves with a complex vegetation-over-soil target. A physically-based modeling approach is essential for analyzing the interaction of crop biological variables and SAR backscatter over a wide range of crop conditions and sensor configurations.

In this study, L- and C-band backscatter at certain polarizations exhibited a strong correlation with LAI. Some of the unexplained error in these simple correlations may be attributable to contributions from the soil moisture. Therefore, the water cloud model was used to model the effect of LAI and surface soil moisture on SAR backscatter.

Data needed to parameterize soil moisture in the water cloud model were available from the *in situ* measurements taken coincident with the RADARSAT-2 and ALOS overpasses. No *in situ* measurements were available for the August 21 TerraSAR-X acquisition. Thus TerraSAR-X data were not implemented into the water cloud model.

For the corn and soybean crops, the mean backscatter was extracted for a 70 x 70 metre area centred on the soil moisture sampling sites. A similar approach was taken to calculate average LAI for each site, from the LAI maps derived from the optical data.

To overcome instability problems caused by possible correlations between parameters, a two-step procedure was taken. The model parameter D defining the radar sensitivity to soil moisture was first determined using an independent data set. Once parameter D was fixed, the remaining parameters A, B, E, and C were then simultaneously determined. Three of the soybean fields were seeded late because of an unusually rainy spring season, and thus for eleven soybean sites, the soybean crop had not yet emerged at the time of the June 12 FQ6 and June 15 FQ20 RADARSAT-2 acquisitions. For the PALSAR/ALOS acquisition on May 23, 2007, soil moisture measurements were taken during the satellite overpass. At that time, most of fields were bare as crops had not yet emerged. Based on these data, a linear regression model was developed to describe the relationship between SAR backscatter and soil moisture in the absence of vegetation. This process was used to determine and fix the parameter D. Next, the remaining parameters in the model, A, B, E and C, were determined using a non-linear least squares method in the Matlab Curve Fitting Toolbox environment, based on the Levenberg-marquardt algorithm.

The degree of model fit was indicated by the coefficient of determination ( $R^2$ ) and RMSE, and these statistics are provided in Table 3.

SAR Backscatter	Corn		Soybeans	
	Coefficient of determination ( $R^2$ )	RMSE (power)	Coefficient of determination ( $R^2$ )	RMSE (power)
PALSAR/ALOS				
HH	0.78	0.013	0.44	0.019
HV	0.81	0.002	0.38	0.005

RADARSAT-2 FQ20				
HH	0.63	0.026	0.10	0.022
HV	0.78	0.004	0.07	0.003
RADARSAT-2 FQ6				
HH	0.26	0.038	0.43	0.019
HV	0.71	0.004	0.38	0.005

Table 3. Statistics describing the fit of the water cloud model to SAR backscatter

A good model fit was achieved for most SAR configurations for corn, with coefficients of determination ( $R^2$ ) reaching 0.63–0.81. The one exception was the poor correlation for C-HH backscatter (RADARSAT-2 FQ6). For soybeans, the water cloud model provided only weak correlations for all SAR frequencies and polarizations. In figure 3, the fitted models using the L-HV backscatter are plotted against the observed data for corn.

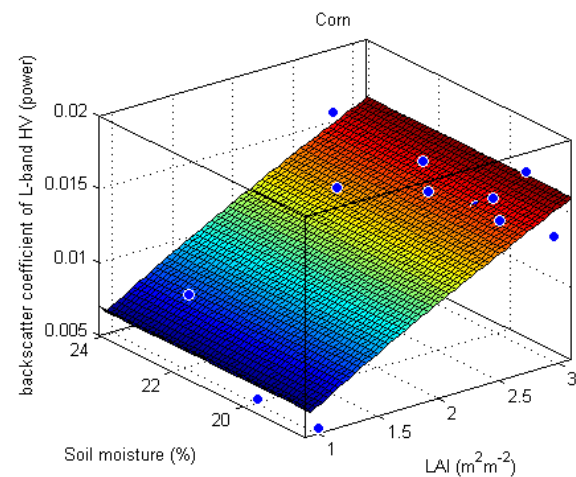


Figure 3. Modeled and observed L-HV backscatter expressed as a function of soil moisture and LAI for corn.

For corn, the highest correlations were again reported for L-band backscatter at HH and HV polarizations. Slightly lower correlations were reported at most C-band polarizations except for C-HH backscatter (RADARSAT-2 FQ6 mode). Backscatter from soybeans, regardless of frequency or polarization, were not significantly correlated with LAI.

## 5. CONCLUSION

This study investigated the relationship between multi-frequency SAR backscatter and LAI for corn and soybean crops. TerraSAR-X dual-polarized stripmap data (X-band), RADARSAT-2 Fine beam quad-polarized data (C-band) and ALOS PALSAR dual-pol data (L-band), as well as optical data including the Compact Airborne Spectrographic Imager (CASI) and SPOT-4 multi-spectral data were acquired during the 2008 crop growing season. SAR backscatter was extracted from each SAR image. LAI maps were derived from the optical images at a detailed pixel level. Object-based segmentation of the LAI maps defined the basic sampling unit upon which mean LAI and SAR responses were calculated.

A statistical correlation analyses quantified the relationship between the SAR parameters and LAI. High correlation coefficients with corn LAI were found for L-band and C-band. The highest correlation coefficients ( $r=0.90$ – $0.96$ ) were reported for L-HH, L-HV and C-HV (RADARSAT-2 FQ6

mode). SAR backscatter was only weakly correlated with soybean LAI. The highest correlations were reported at C-band ( $r=0.58-0.80$ ). X-band backscatter was poorly correlated with both corn and soybean LAI.

The water cloud model was used to parameterize the relationship between LAI and soil moisture, and SAR backscatter at L- and C-band. The correlation between SAR backscatter and LAI didn't show significant improvement following implementation of the model. Further research will couple soil moisture models and/or *in situ* network data with the water cloud model to improve parameterization of the contribution from the underlying soil.

Ulaby, F.T., Allen, C.T., Eger Iii, G. and Kanemasu, E., 1984. Relating the microwave backscattering coefficient to leaf area index. *Remote Sensing of Environment*, 14(1-3): 113-133.

#### REFERENCE

Baret, F. and Guyot, G., 1991. Potentials and limits of vegetation indices for LAI and APAR assessment. *Remote Sensing of Environment*, 35(2-3): 161-173.

Brown, L., Chen, J.M., Leblanc, S.G. and Cihlar, J., 2000. A Shortwave Infrared Modification to the Simple Ratio for LAI Retrieval in Boreal Forests: An Image and Model Analysis. *Remote Sensing of Environment*, 71(1): 16-25.

Chen, J.M. and Cihlar, J., 1996. Retrieving leaf area index of boreal conifer forests using Landsat TM images. *Remote Sensing of Environment*, 55(2): 153-162.

Clevers, J.G.P.W. and van Leeuwen, H.J.C., 1996. Combined use of optical and microwave remote sensing data for crop growth monitoring. *Remote Sensing of Environment*, 56(1): 42-51.

Ferrazzoli, P., Guerriero, L., Quesney, A., Taconet, O.A.T.O. and Wigneron, J.P.A.W.J.P., 1999. Investigating the capability of C-band radar to monitor wheat characteristics. In: L. Guerriero (Editor), *IGARSS 1999, Processings of the International Geoscience and Remote Sensing Symposium*. IEEE, Hamburg, Germany, pp. 723-725.

Haboudane, D., Miller, J.R., Pattey, E., Zarco-Tejada, P.J. and Strachan, I.B., 2004. Hyperspectral vegetation indices and novel algorithms for predicting green LAI of crop canopies: Modeling and validation in the context of precision agriculture. *Remote Sensing of Environment*, 90(3): 337-352.

Liu, J. et al., 2009. Quantifying Crop Biomass Accumulation Using Multi-temporal Optical Remote Sensing Observations, *Proceedings of the 30th Canada Symposium on Remote Sensing*, Lethbridge, Alberta.

McNairn, H.D., V; Murnaghan, K, 2002. The Sensitivity of C-Band Polarimetric SAR to Crop Condition, *IGARSS 2002, Proceedings of the International Geoscience and Remote Sensing Symposium*. IEEE, Toronto, Canada, pp. 1471-1473.

Prévoit, L., Champion, I. and Guyot, G., 1993. Estimating surface soil moisture and leaf area index of a wheat canopy using a dual-frequency (C and X bands) scatterometer. *Remote Sensing of Environment*, 46(3): 331-339.

Taconet, O., Vidal-Madjar, D., Emblanch, C. and Normand, M., 1996. Taking into account vegetation effects to estimate soil moisture from C-band radar measurements. *Remote Sensing of Environment*, 56(1): 52-56.